International Journal of Thin Films Science and Technology

http://dx.doi.org/10.18576/ijtfst/120310

Study the Defect of Organic Electron Transport Materials of Perovskites Solar Cell

Hussein K. Mejbel[1], *Samir M. AbdulAlmohsin*[1,*] *and Dhuha E. Tareq*[2].

[1] Department of Physics, College of Education for Pure Science, ThiQar University, Nasiriyah, Iraq
[2] Department of Biomedical Engineering, College of Engineering, ThiQar University, Nasiriyah, Iraq

Received: 13. May 2023, Revised: 15 Jun. 2023, Accepted: 10 Aug. 2023
Published online: 1 Sep. 2023.

Abstract: In this study, the Organic Perovskite solar cells have been of great interest due to their low cost and great efficiency. The perovskite materials have huge charge carrier mobility with greater stability than organic materials, metal oxides have shown great promise. In this research, because of its improved performance, we used PCBM represent as Electron Transport layer-ETL, NiO is Hole Transport Material (HTM), and $CH_3NH_3PbI_3$ as an absorber. His work is concerned with the design and analysis of lead-based perovskite solar cell model with the versatile FTO/PCBM/$CH_3NH_3PbI_3$/NiO/Pt architecture. Via system simulation, we researched the effects of some parameters on the performance of the solar cell device. Solar cell efficiency was found to be related to the perovskite and PCBM layer thicknesses. The tunable performance of organic perovskite solar cells with the power conversion efficiency (PCE) of 47.49% was reached when a defect of $CH_3NH_3PbI_3$was $1 \times 10\text{^}10$ cm^{-3}, short circuit current density (Jsc) 46.214 mA/cm^2, open-circuit voltage (Voc) 1.397 V, fill factor(FF) 73.52% respectively. These results showed the perovskits solar cell was the best optimal for perovskite solar cells with high stability and efficiency.

Keywords: Perovskits, Organic Semiconductor, Solar Cells.

1 Introduction

Because of its outstanding features such as ideal bandgap, broad absorption range, the good transport mechanism for the carrier, simplicity of manufacturing on the supple substrate, and changeable bandgap, $CH_3NH_3PbI_3$ becomes a good light harvester [1–6]. The above-mentioned characteristics of the lead halide perovskite material encourage the manufacturing use of perovskite solar cells and become a good economical material for the natural silicone material [7–10]. In the launching, the maximum value of PCE for the $CH_3NH_3PbI_3$ perovskite solar cell is 3.8 percent [11]. In due development, using the innovative methods of manufacturing and the suitable range of the architecture the PCE of perovskite solar cell reached PCE of 22.1 percent [12]. The solution method represents cost – production method of Methyl ammonium lead halide perovskite materials which are abundant on the planet. To improve the performance of the device, a very clear thoughtful of the original relationship between the materials characteristics and the device architecture is essentially required. Fullerene derivative (PCBM), fullerene is a molecule made entirely from carbon in the custom of a dull sphere, ellipsoid, or tube. PCBM has excellent electron mobility value, and it has represented the part of electron acceptor mostly in organic solar cells which studied by scientist in this field [12]. E.g. equals the difference between LUMO and HOMO in organic materials. Therefore, the aim of the PV analysis is to seizure all wave length of the incident photons by choosing to conduct large absorption spectroscopy, thus generating several pairs in the multiband semiconductor .Amphoteric defect state of the absorber, defect tolerance at interfaces and electrical properties of the solar cells have also been investigated .Bulk heterostructure tends to improve the separation of the exciton, but electron and hole charge mobility and power conversion efficiency of the collection are affected. In this very complex framework, there is a need to do modeling work that can realistically approximate measurements used in characterizing solar cells. Such a program was developed at the University of Gent, called SCAPS.

Fig. 1: The organic structure of PCBM.[13]

*Corresponding author E-mail: samer75_phy@sci.utq.edu.iq

2. Simulation and Modeling Computer

The principal work of solar cells can produce power electricity due to being exposed to sunlight by a photovoltaic phenomenon, which is a process for both chemical and physical major. When a device solar cell is hit to sun light, only photons have energy greater than energy gap is absorbed by materials of semiconductor. With complete excitation energy, the absorbed photons will cause electrons and holes to be carried; electrons move in the conduction band and holes move in the valence band travel in different directions. Short circuit current density (JSC), open-circuit voltage (VOC), fill factor (FF) and conversion efficiency are the photovoltaic parameters used to determine a photovoltaic system's output (almost). Burgelman et al. generated the SCAPS-1D one-dimensional simulation program. From Gent University, Belgium. SCAPS can calculate by many solar cell-related properties, such as energy gaps, density of state of CB, VB, current density, QE, and J-V. The chart below displays procedures for running SCAPS and its action panel simulation.

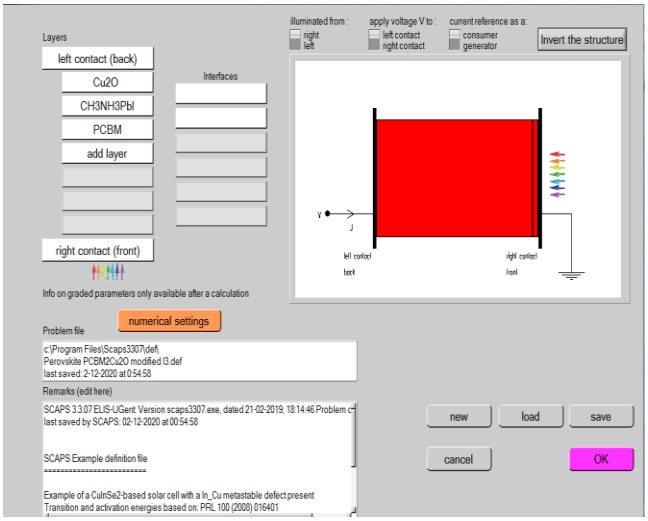

Fig. 2: Drift map and accomplishment panel SCAPS [14].

The Work Method base Flow Chart SCAPS illustrates in what way SCAPS lunches by foundational the action pad. Usual the issue due to enter the layer of the organic perovskite construction to provide input parameters data. Specify the temperature, voltage, frequency, and certain points of the operating state. The defined behavior to be measured is J-V, QE, C-V and C-F, so using SCAPS is run to display simulated plots results of solar cell such as open circuit voltage, short circuit current, etc. Most structures of perovskites are based on FTO/ETL/perovskite/HTL/Pt where the transparent conducting oxide is referred to by the electron transport layer of FTO, ETL, and HTL. The heart of the solar cell is the hole transport materials and the Perovskite semiconductor (Active layer). In Figure 3, the energy bandgap used for this simulation is given.

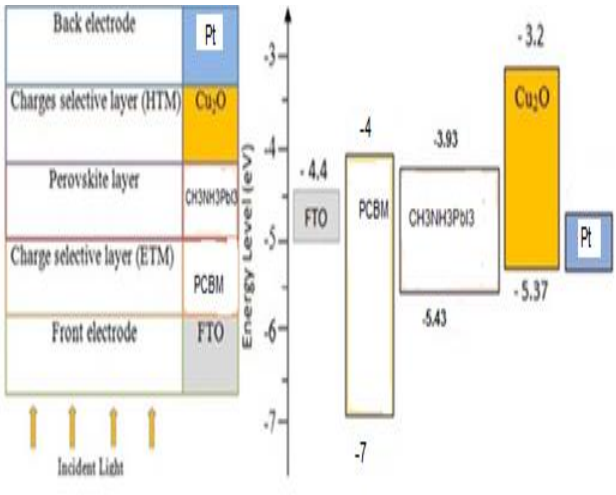

Fig. 3: Typical of simulation building and diagram of energy levels of various perovskites materials

3 Modeling and simulation

The following mathematical Poisson's expressions were extracted by SCAPs-1Dfor modeling and simulation of Cells parameters, characteristics and quantum efficiency which are based on the [15]:

$$\frac{d}{dx^2}\phi_{(x)} = \frac{e}{\varepsilon_0 \varepsilon_r}\left[p_{(x)} - n_{(x)} + N_D - N_A + \rho_P - \rho_n \right] \quad \text{.....(1)}$$

Here ∈r is relative and ∈0 is the vacuum dielectric permittivity, Φ is electrostatic potential, ND, NA, are charged donor, acceptor impurities, and electron charge, ρn and ρp are electrons and holes distribution. continuous equations areas for electrons and holes [16]:

$$\frac{d}{dx} J_n(x) - e\frac{\partial n_{(x)}}{\partial t} - e\frac{\partial n_{(x)}}{\partial t} - e\frac{\partial \rho_n}{\partial t} = G(x) - R(x) \quad \text{.....(2)}$$

$$\frac{d}{dx} J_P(x) + e\frac{\partial p_{(x)}}{\partial t} + e\frac{\partial \rho_P}{\partial t} = G(x) - R(x) \quad \text{.....(3)}$$

Jp,Jn,G(x) and R(x) are holes and electrons densities, generation and recombination rate [16]. This technique lets us calculate the open circuit voltage, current density, quantum efficiency, [16].

Table 1: Summary of parameters used for perovskite SCAPS modeling [17,18,19]

parameters	Cu_2O	$CH_3NH_3PbI_3$	PCBM
Band gap(ev)	2.17	1.5	2
Electron effinity (ev)	3.20	3.9	3.9
Dielectric permittivity	7.11	10	3.9
CB effective density of states (1/cm^2)	2.02E+17	2.75E+18	2.2E+19
VB effective density of states (1/cm^2)	1.10E+19	3.9E+18	2.5E+19
Electron mobility (cm^2/v.s)	2.000E+2	1.00E+1	2E-2
Hole mobility (cm^2/v.s)	8.00E+18	1.0E+1	2E-2

Table 2: solar cells device Parameters used numerical analysis

Left electrical properties (Pt.)	
surface recombinationVelocity of electron (cm/s)	10^5
surface recombinationVelocity of hole (cm/s)	10^7
work function (ev) of Pt	5.65
Right contact electrical properties	
Velocity of electron (cm/s)	10^7
Velocity of hole (cm/s)	10^5
ITO glass , work function ITO (ev)	4.4

4 Result and discussion

1. Effect layer thickness and Temperatures variation on the $Cu_2O/CH_3NH_3PbI_3$/PCBM solar cells

1.1 Effect Cu2O layer thickness on solar cells

The active layer has been established to get the best thickness which absorbs the highest number of photons and to create excitons which are e-h pairs. The thickness of perovskites layer ranged from 0.3µm to 1.8µm. whenever the thickness increase, the longer wavelength of illumination create amount of electron-hole pair generation. The back contact gets very close to depletion layer, by increasing the thickness of the absorber layer, and the back contact collects more electrons for recombination. Via these less electrons, the generation progression will participate and eventually lead to the Voc, Jsc increase, Decreased fill factor, and enhanced performance. The variance of PV parameters with the absorber layer thickness is seen in Figure 4. Due to the increased exciton performance, the graph shows the power conversion efficiency increase as we tune from the thin to thick absorber. But in the fill factor, there is a fast drop.

Table 3: Variant Thickness for Cu_2O with parameters of solar cells

Thickness (µm) Cu_2O	**Voc (V)**	**Jsc (mA/cm2)**	**F.F (%)**	**η (%)**
0.3	0.829	23.875	22.23	4.42
0.8	0.9229	33.966	22.64	7.10
1.300	0.997	36.175	21.29	7.68
1.800	1.049	37.388	20.53	8.06
2.300	1.085	38.209	20.14	8.36
2.800	1.111	38.821	19.95	8.61
3.300	1.131	39.297	19.86	8.83
3.800	1.146	39.690	19.84	9.03
4.300	1.158	40.013	19.86	9.21
4.800	1.168	40.288	19.92	9.38
5.300	1.177	40.535	19.98	9.54
5.800	1.187	40.743	20.07	9.69
6.300	1.191	40.927	20.16	9.83
6.800	1.196	41.091	20.26	9.97
7.300	1.201	41.239	20.37	10.10
7.800	1.206	41.387	20.47	10.22
8.300	1.210	41.509	20.58	10.34
8.800	1.214	41.580	20.71	10.46
9.300	1.217	41.68	20.82	10.57
9.800	1.220	41.752	20.95	10.68
1.300	0.983	35.850	21.52	7.59
1.800	1.049	37.388	20.53	8.06

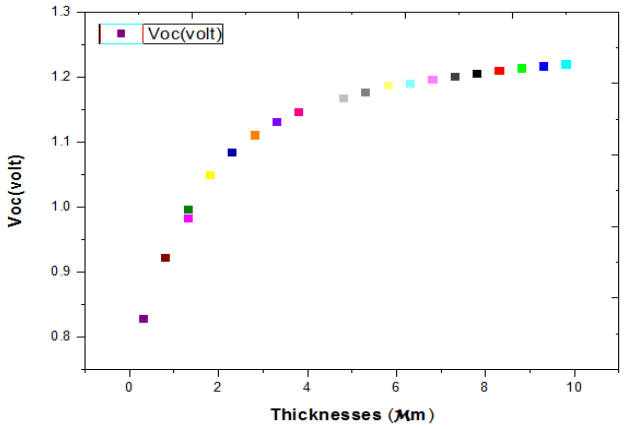

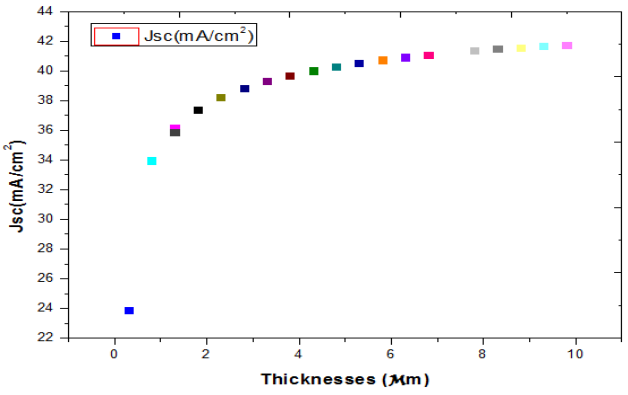

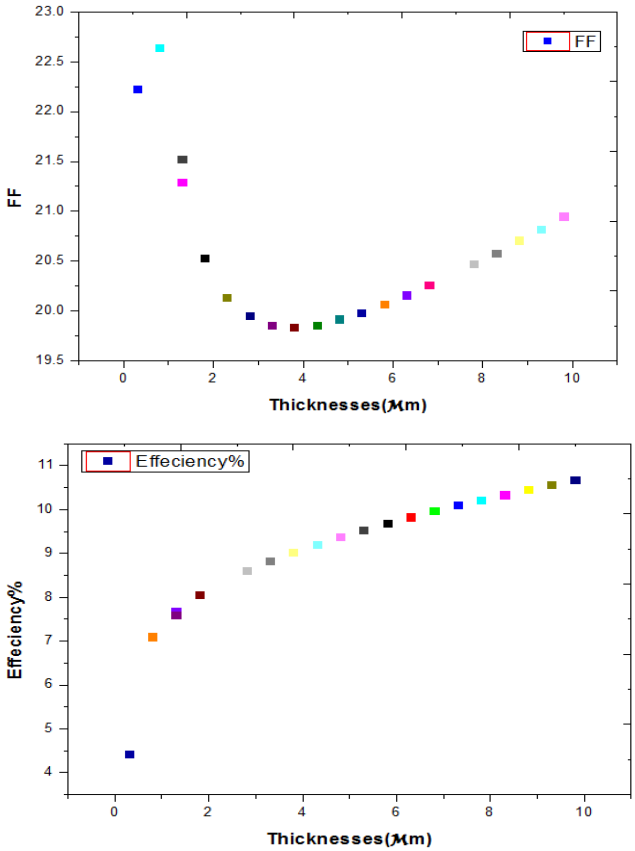

Fig. 4: Variation of PV parameters by thickness variation of Cu_2O.

1.2 Effect of the $CH_3NH_3PbI_3$ layer thickness change on solar cells

The thin film thickness of the perovskits changed from 0.2µm to 0.6µm. Figure 4 shows the change of PV parameters with absorber layer thickness. As we shift from a thin to thick absorber one, the graph shows that efficiency, Voc, and Jsc are decreased. Yet an upgrade is in progress. Table number four displays the sketch figure data. Drawing data shows the optimum thickness for perovskite solar cells which is 0.2 micrometer as listed in table 4 where 0.2-micrometer thickness tallies to the efficiency of (10.77)%.

Table 4: Variation of Thickness for $CH_3NH_3PbI_3$ with device parameters

Thickness (µm) $CH_3NH_3PbI_3$	**Voc (V)**	**Jsc (mA/cm2)**	**F.F (%)**	**η (%)**
0.2	1.220	41.876	21.06	10.77
0.250	1.230	35.001	17.86	7.69
0.3	1.206	26.186	18.62	5.88
0.350	1.165	19.540	21.39	4.87
0.4	1.136	14.967	25.78	4.39
0.450	1.124	11.843	31.25	4.16
0.5	1.120	9.728	37.27	4.06
0.550	1.117	8.344	43.07	4.02
0.6	1.117	7.49	47.73	4

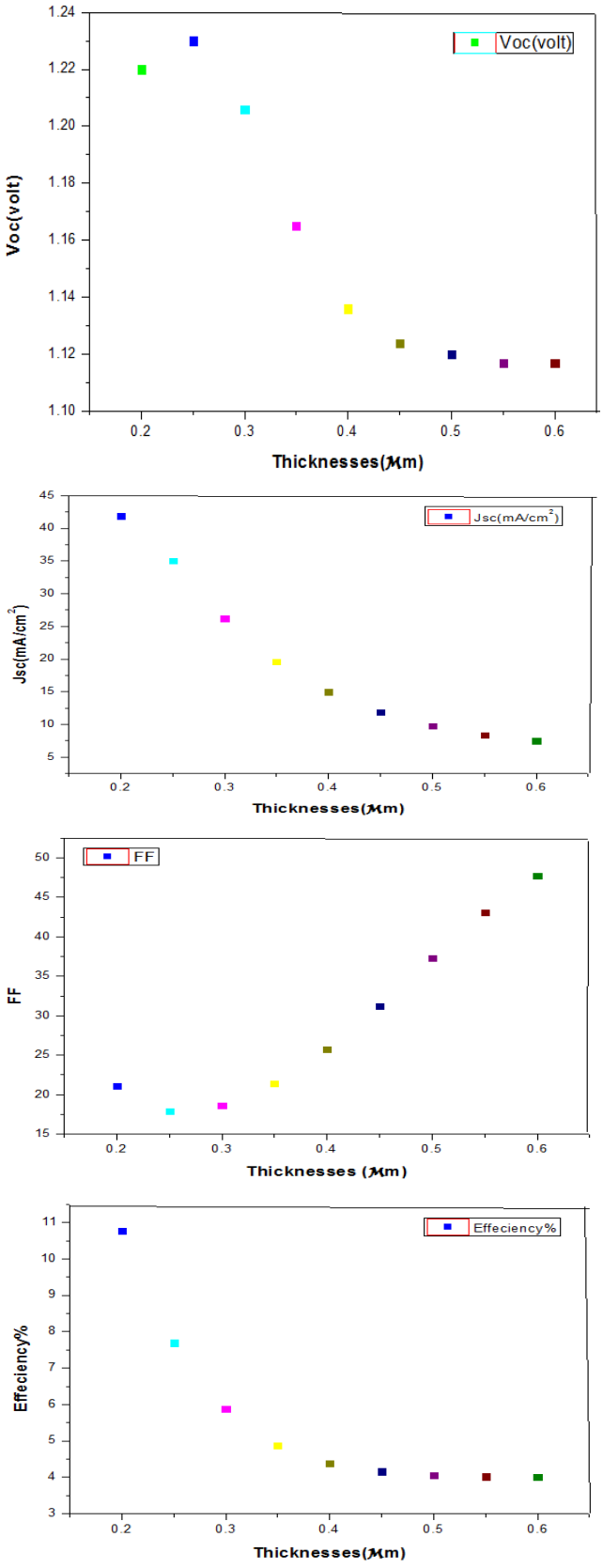

Fig. 5: PV parameters correspond to thickness variation of $CH_3NH_3PbI_3$

1.3 the PCBM layer thickness

The PCBM is currently used as an electron transport material for the Perovskite solar cell. The alignment between the valence band (VB) for both materials ETM and perovskits, conduction band (CB) of the perovskite with PCBM due to its highest occupied molecular orbital (HOMO) and lowest unoccupied molecular orbital (LUMO) levels, allowing for good electron transport to the PCBM layer. At the perovskite-PCBM interface, the blocking of holes occurred due to the lower PCBM HOMO compared to that of the perovskite valence band[20] In this segment, we will analyze the lower PCBM HOMO compared to the perovskite valence band[20] The effect of the PCBM layer's thickness. One indicates that, as shown in table 5, the ideal thickness for perovskite solar cells is 0.01 micrometer, where 0.01 micrometer thickness matches the efficiency of the solar cells of (13.42)%.

Table 5: Variant PCBM thickness with solar cells parameters

Thickness (µm) PCBM	Voc (V)	Jsc (mA/cm2)	F.F (%)	η (%)
0.01	0.746	37.194	42.27	11.73
0.02	0.757	37.472	44.07	12.15
0.03	0.764	37.944	45.33	13.15
0.04	0.766	38.160	45.77	13.40
0.05	0.767	38.142	45.83	13.42
0.06	0.767	38.142	45.83	13.42
0.07	0.767	38.142	45.83	13.42

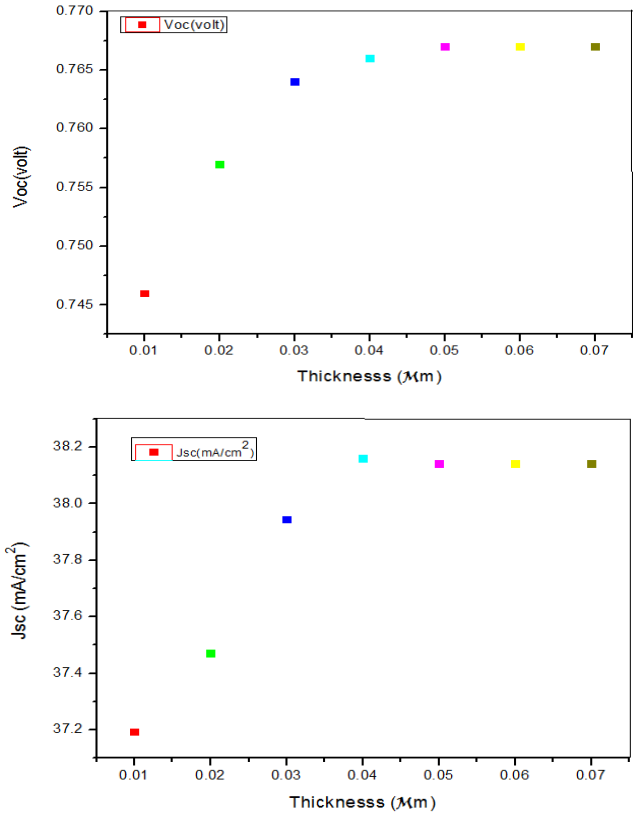

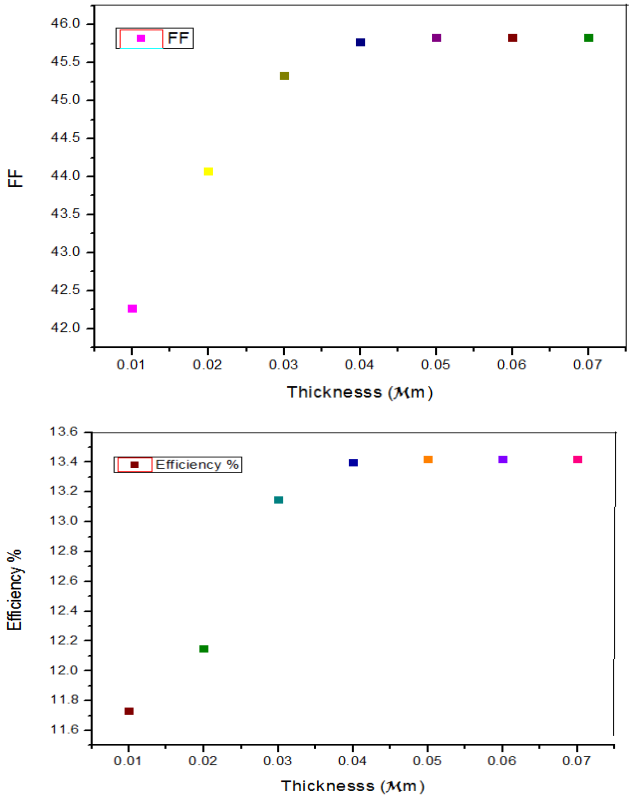

Fig. 6: Variation of PV parameters by adjusting the thickness of PV parameters PCBM

1.4 Effect of annealing temperatures

simulation I-V characteristic results such as Power conversion efficiency(CE), FillFactor , open circuit voltage(Voc), of the perovskite solar cells device with fluctuating temperature as shown in Table 6 where the highest efficiency is 47.49% and the other important parameter such as Jsc=46.214 mA/cm2, FF 73.52= % and Voc =1.397 is achieved at the temperature of 333.15 K, Consequently, the best outcome at very high levels The temperature is appropriate for working in a vacuum. When the temperature is decreased, Due to the decrease in the generation of electron-hole pairs in the perovskite materials with increasing temperature, the PCE, Voc and Jsc degrees are from 333.15 K to 233.15 K, as shown in Illustration. The open-circuit voltage steadily decreases with a decrease in Figure 7. Due to the regulation of the temperature, the performance can be modified by temperature.

Table 6: The parameter of the Cu_2O/ CH3NH3PbI3/PCBM heterojunction solar cell

Temperature (K)	Voc (V)	Jsc (mA/cm2)	F.F (%)	η (%)
333.15	1.397	46.214	73.52	47.49
313.15	1.279	46.214	71.74	42.42
293.15	1.162	46.214	70.89	38.09
273.15	1.056	46.213	71.19	34.77
253.15	0.974	46.205	70.73	31.85
233.15	0.907	46.121	68.80	28.79

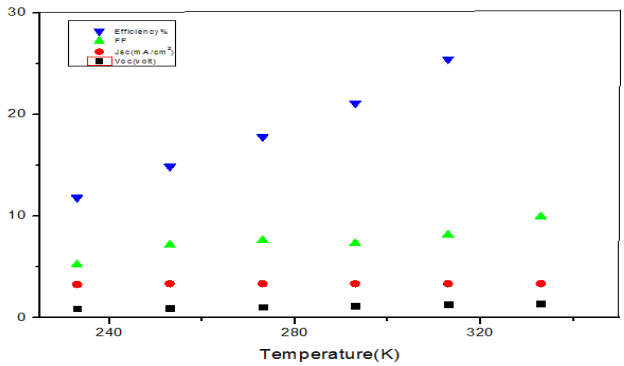

Fig. 7: solar cell parameters with the temperature.

1.5 Defect State of the Interface Layer ($Cu_2O/CH_3NH_3PbI_3$/PCBM).

defect layer has been considered for the simulations of the proposed $CH_3NH_3PbI_3$ solar cell structures. The study has been simulating numerically for the defect density of state from 1×10^{10} cm^{-3} to $1 \times 10^{18} cm^{-3}$. Fig 8displays the result of defect density versus Isc, Voc, FF, and efficiency for Cu2O/CH3NH3PbI3/PCBM solar cells. the graphs show that, the Voc, Jsc, FF, and η falling with growing defect density. When the defect density increases up to $1 \times 10^{18} cm^{-3}$, a decline in efficiency is detected. With growing defect density, the recombination rate also rises which in turn decreases the efficiency. So, it can be understood that the results of defect density of 1×10^{10} cm^{-3} is best for device simulation(η=47.49%).

Table 7: Variation of defect for Cu2O/CH3NH3PbI3/PCBM with device parameters

Defect Nt(1/cm^3)	Voc (V)	Jsc (mA/cm2)	F.F (%)	η (%)
1*10^{10}	1.397	46.214	73.52	47.49
1*10^{11}	1.279	46.214	71.74	42.42
1*10^{12}	1.162	46.214	70.89	38.09
1*10^{13}	1.056	46.213	71.19	34.77
1*10^{14}	0.974	46.205	70.73	31.85
1*10^{15}	0.907	46.121	68.80	28.79
1*10^{16}	0.842	45.296	36.31	24.17
1*10^{17}	0.766	38.160	45.77	13.40
1*10^{18}	0.667	12.241	29.23	2.39

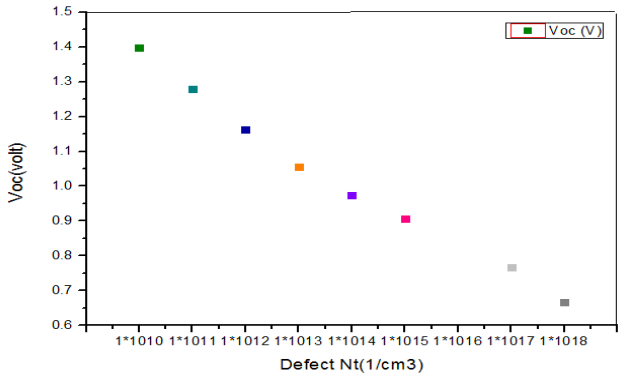

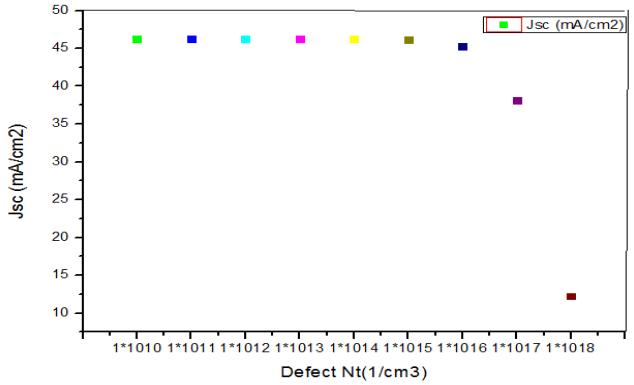

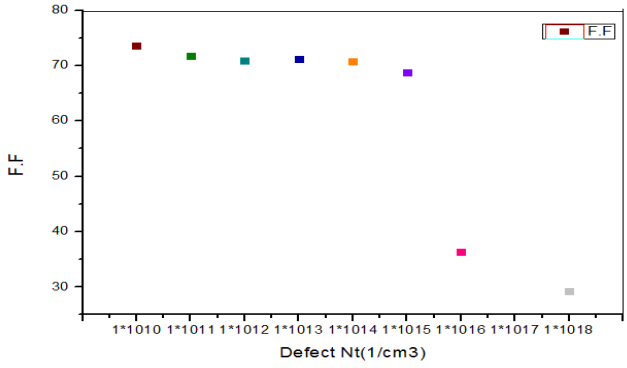

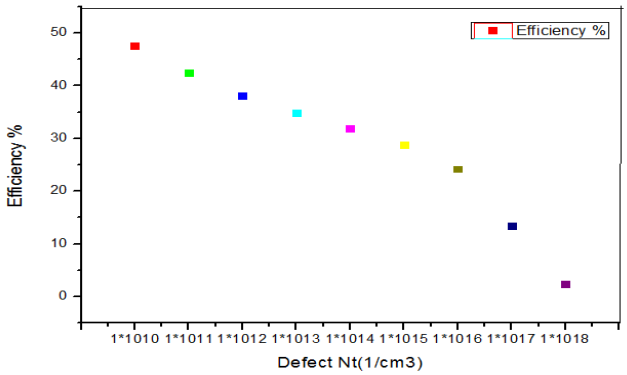

Fig. 8: Defect density of the HTM/$CH_3NH_3PbI_3$/ETM layer.

1.6. Effects of the CB,VB density of State of the ($Cu_2O/CH_3NH_3PbI_3$/PCBM).

A higher density of localized states decreases the quasi-Fermi level separation and contributes to lower Voc values. In relation to the Voc value, the effect of carrier mobility is less direct since there is now direct current extraction in open-circuit conditions. The mobility of the carrier will affect the recombination process, which must equal the rate of generation in open-circuit and steady recombination. Due to the lower carrier mobility, the Voc decreases due to a higher density of states along with Jsc and FF values. [21]. The optimum efficiency value depends on the density of states for CB & VB (Fig 9 and 10). The highest values of Jsc, FF and η % were found at CB=1*10^{19},VB=1*10^{20}. The Voc also reduction with rise in the CB and VB density of states from 1.339 to 1.187 v and obtain high efficiency at CB=1*10^{19}, η= 45.44 % and VB=1*10 ^{20}, η=42.83%.

Table 8: Variation of CB for Cu_2O/ $CH_3NH_3PbI_3$/PCBM with device parameters

CB	Voc (V)	Jsc (mA/cm2)	F.F (%)	η (%)
$1*10^{19}$	1.339	46.746	72.59	45.44
$1*10^{20}$	1.280	46.786	72.02	43.15
$1*10^{21}$	1.230	46.798	68.46	39.54
$1*10^{22}$	1.204	43.879	51.26	27.10
$1*10^{23}$	1.194	25.356	39.50	11.96
$1*10^{24}$	1.187	9.397	37.74	4.21

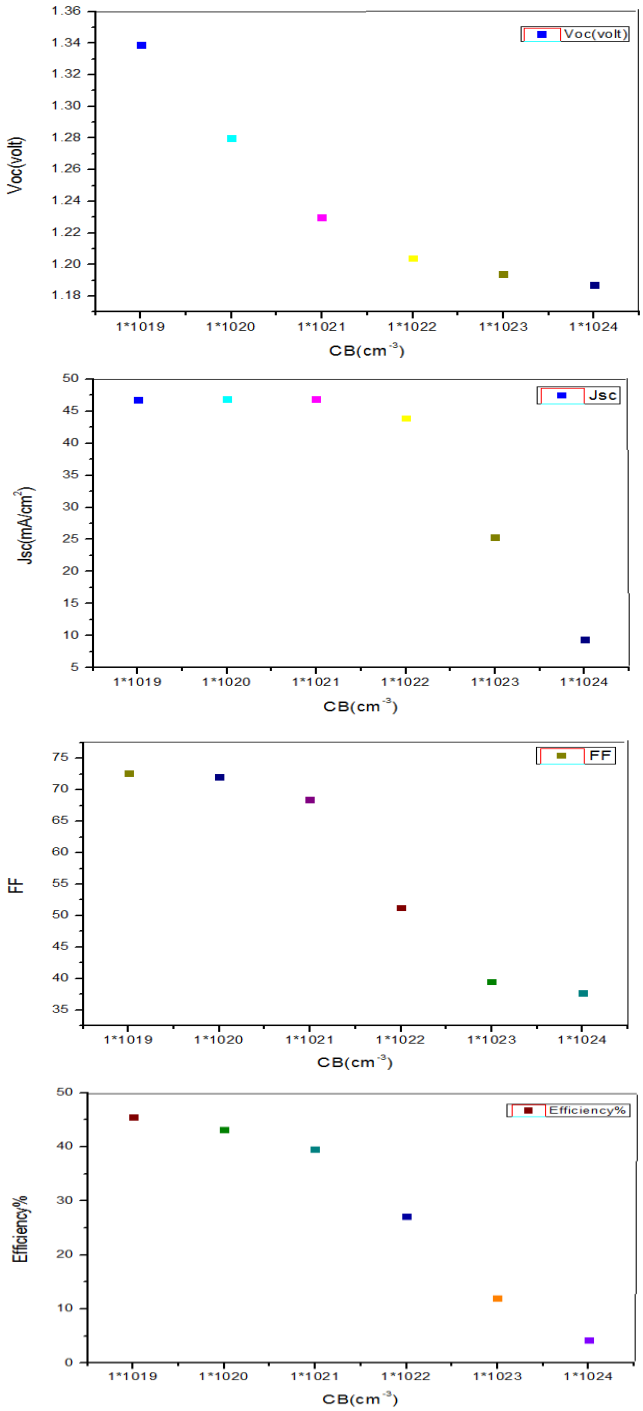

Fig. 9: CB density of the HTM/$CH_3NH_3PbI_3$/ETM layer

Table 9: Variation of CB for Cu_2O/$CH_3NH_3PbI_3$/PCBM with device parameters

VB	Voc (V)	Jsc (mA/cm2)	F.F (%)	η (%)
$1*10^{20}$	1.280	46.78	71.52	42.83
$1*10^{21}$	1.220	46.799	70.39	40.70
$1*10^{22}$	1.160	46.805	69.15	37.57
$1*10^{23}$	1.101	46.806	67.80	34.95
$1*10^{24}$	1.041	46.807	66.33	32.33
$1*10^{25}$	0.981	46.807	64.70	29.74
$1*10^{26}$	0.922	46.807	62.91	27.15

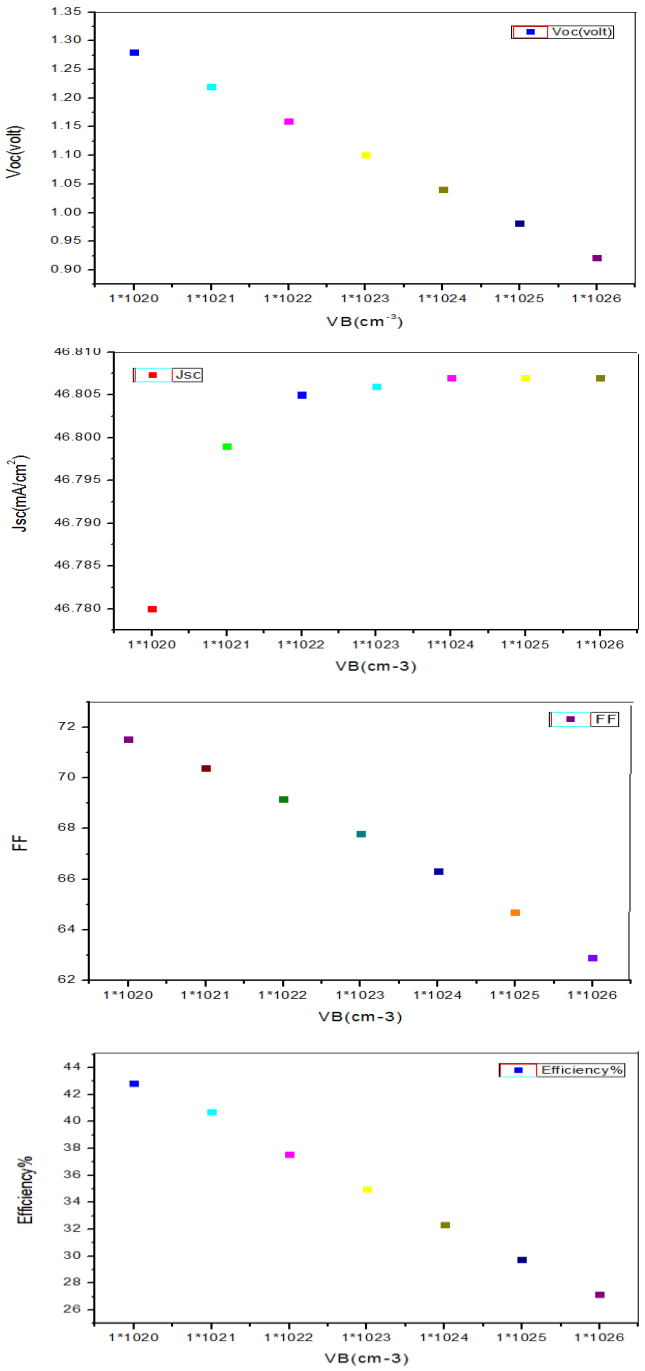

Fig. 10: VB density of the HTM/$CH_3NH_3PbI_3$/ETM layer

5 Conclusions

It can conclude that , the thickness have been changed for PCBM, NiO,and CH3NH3PbI3 were studied in each semiconductor substance and after in addition to change with a variation of degree of temperature and defect state to catch tunable condition searching for greatest efficiency of the device NiO/CH3NH3PbI3/PCBM solar cells which reached around 47 % which is best device perovskites structure and highest efficiency comparing with the device of NiO/CH3NH3PbI3/PCBM solar cells reaches also around 47% at defect $1*10^{10}Nt(cm^{-3})$, in addition to that all rest of parameter device enhanced as result to use PCBM as electron transport materials, and NiO as Hole transport layer.

Acknowledgments

We would like to thank mark burger man, the electronic and information system (Elis), the university of gent, Belgium, for providing us the free access to SCAPS simulation software, and supervisor Samir M. Abdul Almohsin ThiQar University, supervisor Hussien-hade ThiQar University.

References

[1] Dong Q, Fang Y, Shao Y, Mulligan P, Qiu J, Cao L, Huang J. Electron-hole diffusion lengths 175 mm in solutiongrown CH3NH3 PbI3 single crystals. Science. 2015; 347(6225):968–70.

[2] Chen Y, Peng J, Diqing S, Chen X, Liang Z. Efficient and balanced charge transport revealed in planar perovskite solar cells. ACS Applied Materials and Interfaces. 2015; 7(8):4471–5.

[3] Hsiao YC, Wu T, Li M, Liu Q, Qin W, Hu B. Fundamental physics behind high-efficiency organic-metal-halide perovskite solar cells. Journal of Material Chemistry A. 2015; 3(30):15372–85.

[4] Luo S, Daoud WA. Recent progress in organic-inorganic halide perovskite solar cells: Mechanisms and material design. Journal of Material Chemistry A. 2015; 3(17):8992– 9010.

[5] Mola GT. Enhanced photon harvesting in OPV using an optically reflective surface. Applied Physics. Materials Science and Processing. 2015; 118(2):425–29.

[6] Tessema G. Charge transport across the bulk-heterojunction organic thin film. Applied Physics. A Materials Science and Processing. 2012; 106(1):53–7.

[7] Kazim S, Nazeeruddin MK, Grätzel M, Ahmad S. Perovskite as light harvester: A game changer in photovoltaic's. AngewandteChemie International Edition. 2014 Mar 10; 53(11):2812–24.

[8] Wash Q, Yesmin AJ, Gloria MD, Tashfiq M, Hossain MI, Islam SN. Optical analysis in CH3NH3PbI3 and CH3NH3PbI2Cl based thin-film perovskite solar cell. American Journal of Energy Research. 2015; 3(2):1924.

[9] Won LS, Kim S, Bae S, Cho K, Chung T, Mundt LE, Lee S, Park S, Park H, Martin CS, Stefan WG, Yohan K, Jun Y, Kang Y, Lee HS, Kim D. UV degradation and recovery of perovskite solar cells. Scientific Reports. 2016; 6(38150):1–10.

[10] Yin WJ, Shi TT, Yan YT. Unusual defect physics in CH3NH3PBI3 perovskite solar cell absorber. Applied Physics Letters A. 2014 Feb; 104(6):063903-1–4.

[11] Kojima A, Kenjiro T, Shirai Y, Miyasaka T. Organometal halide perovskites as visible-light sensitizers for photovoltaic cells. Journal of American Chemical Society. 2009; 131(17):6050–51.

[12] NREL [Internet]. [cited 2017 Jan 05]. Available from: groups [Peet*et al.*, 2007; Li *et al.*, 2005; Hoppe *et al.*, 2004]

[13] AHMAD PUAAD OTHMAN School of Applied Physics Faculty of Science and Technology UniversitiKebangsaan Malaysia 43600 UKM Bangi, Selangor, Malaysia puaad@ukm.my

[14] Anish. M., Fabian. B., Jesper. G. A., Fredrik. H., (2016). "A review of solar Energy Based heat and power generation Systems", Renewable and Sustainable Energy Reviews, vol. 67, pp. 1047–1064, 2017

[15] Kumar, Atul, and Ajay D. Thakur. "Analysis Of SnS2 Buffer Layer And SnS Back Surface Layer Based CZTS Solar Cells Using SCAPS." arXiv preprint arXiv:1510.05092 (2015).

[16] Movla, Hossein. "Optimization of the CIGS based thin-film solar cells: Numerical simulation and analysis." Optik 125, no. 1 (2014): 67-70.

[17] D. Wang, H. Cui, G. Su, A modeling method to enhance the conversion efficiency by optimizing light-trapping structure in thin-film solar cells, Sol. Energy 120 (2015) 505–513 https://doi.org/10.1016/j.solener.2015.07.051.

[18] Mohammad I. Hossain, Fahad H. Alharbi, NouarTabet Qatar Environment & Energy Research Institute, Doha, Qatar Received 19 May 2015; received in revised form 6 July 2015; accepted 24 July 2015 Available online 14 August 2015

[19] Hu, L., Peng, J., Wang, W., Xia, Z., Yuan, J., Lu, J., Huang, X., Ma, W., Song, H., Chen, W., Cheng, Y.B., Tang, J., 2014. Sequential deposition of CH3NH3PbI3 on planar NiO film for efficient planar perovskite solar cells. ACS Photonics 1, 547–553. http://dx.doi.org/10.1021/ph5000067.

[20] Malinkiewicz, O., Yella, A., Lee, Y.H., Espallargas, G.M., Graetzel, M., Nazeeruddin, M.K., Bolink, H.J., 2013. Perovskite solar cells employing organic charge-transport layers. Nat. Photon. 8, 128–132. http://dx.doi.org/10.1038/nphoton.2013.341.

[21] Y.R. Galindo-Luna, J. Ibarra-Bahena, R.J. Romero, L. Velazquez-Avelar, C.V. Valdez-Morales, Evaluation of the thermodynamic effectiveness of a plate heat exchanger integrated into an experimental single-stage heat transformer operating with Water/Carrol mixture, Exp. Therm Fluid Sci. 51 (2013) 257–263.